# Leukocyte-associated immunoglobulin-like receptor 1 promotes tumorigenesis in RCC

KENTARO JINGUSHI[1], MOTOHIDE UEMURA[1,2], KOSUKE NAKANO[2], YUJIRO HAYASHI[2], CONG WANG[2], YU ISHIZUYA[2], YOSHIYUKI YAMAMOTO[2], TAKUJI HAYASHI[2], TOSHIRO KINOUCHI[2], KYOSUKE MATSUZAKI[2], TAIGO KATO[2], ATSUNARI KAWASHIMA[2], TAKESHI UJIKE[2], AKIRA NAGAHARA[2], KAZUTOSHI FUJITA[2], KOJI UEDA[3], KAZUTAKE TSUJIKAWA[4] and NORIO NONOMURA[2]

Departments of [1]Therapeutic Urologic Oncology and [2]Urology, Osaka University, Graduate School of Medicine, Suita, Osaka 565-0871; [3]Project for Personalized Cancer Medicine, Cancer Precision Medicine Center, Japanese Foundation for Cancer Research, Koto-ku, Tokyo 135-8550; [4]Laboratory of Molecular and Cellular Physiology, Graduate School of Pharmaceutical Sciences, Osaka University, Suita, Osaka 565-0871, Japan

Received July 19, 2018; Accepted November 12, 2018

DOI: 10.3892/or.2018.6875

**Abstract.** Renal cell carcinoma (RCC) is the most common type of kidney cancer in adults, responsible for approximately 90-95% of cases. We previously reported a novel method that enables direct extraction of extracellular vesicles (EVs) from surgically resected viable tissues, yielding what we term tissue-exudative extracellular vesicles (Te-EVs). Quantitative LC/MS analysis identified 3,871 proteins in Te-EVs, among which leukocyte-associated immunoglobulin-like receptor 1 (LAIR1) was highly enriched in tumor Te-EVs. In the present study, we found that LAIR1 was significantly upregulated in clinical specimens of human RCC tumor tissues compared to that noted in adjacent non-cancerous renal tissues as determined by quantitative PCR analysis. LAIR1 overexpression resulted in accelerated cell proliferation and tumor growth in RCC cells. Moreover, knockdown of LAIR1 using siRNA significantly inhibited cell proliferation in RCC cells. Mechanistically, LAIR1 upregulated the phosphorylation status of Akt, which in turn increased cell proliferation in RCC cells. In clinical RCC specimens, RCC patients with high LAIR1 mRNA expression showed poor progression-free survival compared to those with low LAIR1 expression. These findings indicate that LAIR1 promotes tumorigenesis in RCC.

*Correspondence to:* Dr Motohide Uemura, Department of Therapeutic Urologic Oncology, Osaka University, Graduate School of Medicine, 2-2 Yamadaoka, Suita, Osaka 565-0871, Japan
E-mail: uemura@uro.med.osaka-u.ac.jp

*Abbreviations:* EVs, extracellular vesicles; Te-EVs, tissue-exudative extracellular vesicles; RCC, renal cell carcinoma; LAIR1, leukocyte-associated immunoglobulin-like receptor 1

*Key words:* leukocyte-associated immunoglobulin-like receptor 1, LAIR1, renal cell carcinoma, tissue-exudative extracellular vesicles

## Introduction

Renal cell carcinoma (RCC) is the leading cause of cancer-related death among all urological malignancies (1). Early-stage RCC is usually curable by surgical resection, but a large number of early-stage RCC cases are asymptomatic, with approximately one-third of all patients presenting with metastatic cancer at the time of diagnosis (2,3). Therefore, a better understanding of the molecular mechanisms of RCC progression is crucial for the discovery of novel prognostic markers and targeted therapies.

Extracellular vesicles (EVs), including exosomes, microvesicles and apoptotic bodies, are released by almost all cell types, including tumor cells. Recently, EVs have been shown to play an important role in the development of cancer, facilitating cell-cell communication between cancer cells and the surrounding microenvironment (4). However, previous EV-related studies have mainly focused on exosomes derived from cultured cells. Therefore, to understand cancer-associated EV functions in the human body, we obtained EVs from freshly resected RCC tissue (tumor and adjacent normal renal tissue) by means of a brief incubation in serum-free medium, yielding what we term tissue-exudative extracellular vesicles (Te-EVs) (5). Quantitative LC/MS analysis revealed 106 RCC-specific Te-EV proteins. Among the 106 upregulated proteins, we focused on leukocyte-associated immunoglobulin-like receptor 1 (LAIR1) as a novel cancer-associated EV protein.

LAIR1 is a type I transmembrane glycoprotein of 287 amino acids containing a single extracellular C2-type Ig-like domain and two immunoreceptor tyrosine-based inhibitory motif (ITIMs) in its cytoplasmic tail (6). LAIR1 is expressed on almost all cells of the immune system including natural killer (NK) cells, T cells, B cells and monocytes,

monocyte-derived dendritic cells, eosinophils, and basophils and mast cells (6-10). LAIR1 can inhibit T-cell receptor complex (TCR) mediated signals, possibly via the recruitment of Csk, the SH2 domain-containing protein tyrosine phosphatases SHP-1 or SHP-2, and to a certain extent on signaling through p38 and Erk (11). Unlike other immune-inhibitory receptors such as PD-1 or CTLA4, the functional ligands of LAIR1 are collagens, which upon binding to LAIR1 inhibit immune cell activation (12). However, to the best of our knowledge, no reports have investigated the expression and function of LAIR1 in RCC.

In the present study, we found that LAIR1 was significantly upregulated in RCC tissues compared to that noted in the normal renal tissues. LAIR1 overexpression promoted cell proliferation by upregulating Akt phosphorylation in RCC cells *in vitro*. Moreover, LAIR1 overexpression accelerated *in vivo* tumor growth in a mouse xenograft model. To the best of our knowledge, this is the first report showing that overexpression of LAIR1 contributes to RCC progression.

## Materials and methods

*Chemicals and antibodies*. Monoclonal anti-CD9 antibody (clone 12A12), monoclonal anti-CD63 antibody (clone 8A12) and monoclonal anti-CD81 antibody (clone 12C4), which were previously confirmed to have high specificity for their targets (13,14), were purchased from Cosmo Bio Co., Ltd. (Tokyo, Japan). Monoclonal anti-LAIR1 antibody (cat. no. ab14826) and polyclonal anti-mouse IgG (20 nm gold) preadsorbed antibody (cat. no. ab27242) were purchased from Abcam (Burlingame, CA, USA). Polyclonal anti-LAIR1 antibody (cat. no. HPA011155), monoclonal anti-β-actin antibody (cat. no. A2228) and LY294002 were purchased from Sigma-Aldrich (Merck KGaA, Darmstadt, Germany). Monoclonal anti-pErk1/2 (cat. no. 4370), anti-Erk1/2 (cat. no. 4695), anti-pAkt (cat. no. 4060), anti-Akt (cat. no. 4691), anti-pS6 kinase (cat. no. 9234) and anti-S6 kinase (cat. no. 9202) were purchased from Cell Signaling Technology, Inc. (Danvers, MA, USA). The C terminal FLAG-tagged LAIR1 inserted into pcDNA3.1 (pcDNA3.1/LAIR1-FLAG) was purchased from GenScript Biotech Corp. (Township, NJ, USA).

*Clinical specimens*. The RCC specimens (total 95 paired samples) were obtained from patients undergoing primary resection at the Osaka University Medical Hospital (Osaka, Japan) between 2002 and 2011. Tumor-associated normal renal tissue was also obtained from a subset of these patients when possible. There were no cases with multiple tumors in the present study. Histological diagnosis was established with standard hematoxylin and eosin-stained sections by two senior pathologists experienced in RCC diagnosis. Tumors were staged according to the 6th AJCC TNM staging system (https://cancerstaging.org/references-tools/deskreferences/Pages/default.aspx) and graded according to Fuhrman's nuclear grading system (15). Written informed consent was obtained from each patient, and the study was approved by the ethics review board of the Osaka University Medical Hospital. The pathological information for the clinical tissue is documented in Table I.

*Purification of extracellular vesicles*. Purification of Te-EVs was performed according to the method of Jingushi *et al* (5). In brief, following excision, the tissue samples were immediately immersed in 4 ml Dulbecco's modified Eagle's medium (DMEM) (Wako Pure Chemical Industries, Ltd., Tokyo, Japan) without fetal bovine serum (FBS; Thermo Fisher Scientific, Inc., Waltham, MA, USA) and stored at 4˚C for 1 h. Tissue-immersed medium was then centrifuged at 2,000 x g for 30 min, and the collected supernatants were subjected to the ultracentrifuge method for recovery of Te-EVs. The protein concentration of the obtained tissue-exudative EVs was measured using Micro BCA Protein Assay kit (Thermo Fisher Scientific, Inc.).

For purification of EVs from cell cultured conditioned medium (CM-EVs), RCC cell lines (renal cell carcinoma: 786-O; clear cell renal cell carcinoma: Caki-1; papillary renal cell carcinoma: Caki-2 and ACHN) were seeded into three 10-cm dishes ($5.0x10^5$ cells/dish) and incubated for 48 h. Cells in cultured medium (RPMI-1640) were then centrifuged at 2,000 x g for 30 min, then at 16,000 x g for 30 min, and the collected supernatants were subjected to the ultracentrifuge method for recovery of EVs. The protein concentration of the obtained CM-EVs was measured using the Micro BCA Protein Assay kit (Thermo Fisher Scientific, Inc.).

*Liquid chromatography-tandem mass spectrometry (LC/MS) analysis*. The EV-containing eluates of EVSecond columns (GL Sciences, Tokyo, Japan) were dried and resolved in 20 mM HEPES-NaOH (pH 8.0), 12 mM sodium deoxycholate and 12 mM sodium N-lauroyl sarcosinate. Following reduction with 20 mM dithiothreitol (DTT), at 100˚C for 10 min and alkylation with 50 mM iodoacetamide at ambient temperature for 45 min, proteins were digested with 5 $\mu$l of immobilized trypsin (Thermo Fisher Scientific, Inc.) with shaking at 1,000 rpm at 37˚C for 6 h. After removal of sodium deoxycholate and sodium N-lauroyl sarcosinate by ethyl acetate extraction, the resulting peptides were desalted by Oasis HLB $\mu$Elution plate (Waters Corp., Milford, MA, USA) and subjected to mass spectrometric analysis. Peptides were analyzed by LTQ-Orbitrap-Velos mass spectrometer (Thermo Fisher Scientific, Inc.) combined with UltiMate™ 3000 RSLCnano-flow HPLC system (Thermo Fisher Scientific, Inc.). Protein identification and quantification analysis were performed with MaxQuant software (https://www.biochem.mpg.de/5111795/maxquant). The MS/MS spectra were searched against the *Homo sapiens* protein database in SwissProt, with a false discovery rate set to 1% for both peptide and protein identification filters. Only 'Razor+unique peptides' were used for the calculation of relative protein concentration. For Te-EV protein cargo analysis, all detected peaks were standardized by adjusting the median value to $1.0x10^4$.

*Western blot analysis*. Cells were lysed with Laemmli SDS sample buffer containing 5% 2-mercaptoethanol. EV samples were lysed with Laemmli SDS sample buffer with or without 2-mercaptoethanol. Protein samples were separated on a 7.5-15% sodium dodecyl sulphate (SDS)-polyacrylamide gel electrophoresis (PAGE) gel and then transferred to a polyvinylidene difluoride (PVDF) membrane using the Bio-Rad semi-dry transfer system (Bio-Rad-Laboratories, Hercules,

Table I. Features of the ccRCC clinical samples used in the different analyses.

A, LAIR1 mRNA expression as examined in 30 matched-pair ccRCC clinical samples by qPCR (Fig. 1D)

| | |
|---|---|
| Age (years) | |
| Mean | 61.5 |
| Range | 27-86 |
| Sex | |
| Male | 22 |
| Female | 8 |
| Maximum tumor diameter (mm) | |
| Median | 41 (21-160) |
| TNM classification | |
| I | 18 |
| ≥II | 12 |
| Pathological grade | |
| ≤G2 | 17 |
| ≥G3 | 13 |
| Pathological stage | |
| ≤pT1b | 19 |
| ≥pT2a | 11 |

B, ccRCC clinical samples used for overall survival analysis (Fig. 5A)

| | |
|---|---|
| Age (years) | |
| Mean | 65 |
| Range | 34-82 |
| Sex | |
| Male | 44 |
| Female | 21 |
| LAIRI mRNA expression | |
| High | 21 |
| Low | 44 |
| Maximum tumor diameter (mm) | |
| Median | 70 (40-130) |
| TNM classification | |
| I | 20 |
| II | 10 |
| III | 20 |
| IV | 15 |
| Pathological grade | |
| G1 | 5 |
| G2 | 43 |
| G3 | 17 |
| Pathological stage | |
| pT1 | 21 |
| pT2 | 15 |
| pT3 | 28 |
| pT4 | 1 |

Table I. Continued.

C, ccRCC samples used for progression-free survival analysis (Fig. 5B)

| | |
|---|---|
| Age (years) | |
| Mean | 68 |
| Range | 44-82 |
| Sex | |
| Male | 36 |
| Female | 16 |
| LAIRI mRNA expression | |
| High | 17 |
| Low | 35 |
| Maximum tumor diameter (mm) | |
| Median | 68 (40-130) |
| TNM classification | |
| I | 20 |
| II | 9 |
| III | 20 |
| IV | 3 |
| Pathological grade | |
| G1 | 5 |
| G2 | 36 |
| G3 | 11 |
| Pathological stage | |
| pT1 | 21 |
| pT2 | 10 |
| pT3 | 21 |

LAIR1, leukocyte-associated immunoglobulin-like receptor 1; ccRCC, clear cell renal cell carcinoma; TNM, Tumor, Node, Metastasis.

CA, USA) (1 h, 12 V). Immunoreactive proteins made to react with the antibodies previously described (1:1,000 dilution) were visualized by treatment with a detection reagent (ECL Prime Western Blotting Retection reagent; GE Healthcare, Chicago, IL, USA). Densitometric analysis was performed using the NIH ImageJ software (version 1.51v; NIH; National Institutes of Health, Bethesda, MD, USA).

*Transmission electron microscope (TEM) analysis.* TEM analysis was performed according to the method of Lässer *et al* (16). EV samples (1 $\mu$g) were placed on a formvar carbon-coated nickel grid for 1 h. EVs were fixed with 2% paraformaldehyde and then incubated with the primary antibodies (1:500 dilution) at room temperature for 1 h. Immunoreactive EVs were labeled with the secondary (anti-mouse IgG) antibody preadsorbed onto 20 nm gold nanoparticles and visualized (magnification, x25,000) with the Hitachi H-7650 transmission electron microscope (Hitachi Ltd., Tokyo, Japan).

*qPCR for LAIR1 mRNA expression.* Total RNA was isolated using TRIzol reagent (Invitrogen; Thermo Fisher

Scientific, Inc.). PrimeScript RT Reagent kit (Takara Bio, Inc., Otsu, Japan) was used to prepare cDNA from 500 ng total RNA. The LightCycler® 96 System (Roche, Rotkreuz, Switzerland) was used for qPCR analysis. Thermal cycling conditions for LAIR1 included an initial step at 95˚C for 30 sec, followed by 40 cycles of 95˚C for 15 sec, 60˚C for 15 sec, and 72˚C for 15 sec. Thermal cycling conditions for GAPDH included an initial step at 95˚C for 30 sec, followed by 40 cycles of 95˚C for 15 sec, 59˚C for 30 sec, and 72˚C for 15 sec. Primer sequences for gene amplification were as follows: LAIR1 forward, 5'-CCTGACCTGGCTGTTGAT GTTCT-3' and reverse, 5'-GCCCGGGCTGTCCTCTGT-3'; GAPDH forward, 5'-CCATCACCATCTTCCAGGAG-3' and reverse, 5'-AATGAGCCCCAGCCTTCTCC-3'.

*Immunohistochemistry*. The expression of LAIR1 was determined by immunohistochemical staining of paraffin-embedded tissues of normal kidney or RCC. Formalin-fixed paraffin-embedded sections (5-$\mu$m in thickness) were deparaffinized and rehydrated. After the slides were steamed for 20 min in 10 mmol/l citrate buffer (pH 6.0) for antigen retrieval, endogenous peroxidase was blocked using 3% $H_2O_2$. Immunohistochemical staining for LAIR1 was performed using anti-LAIR1 (dilution 1:500; cat. no. HPA011155; Atlas Antibodies, Romma, Sweden) and the EnVision+ Detection System (Dako; Agilent Technologies, Inc., Santa Clara, CA, USA), according to the manufacturer's instructions. Primary antibodies were incubated overnight at 4˚C and counter-stained with hematoxylin.

*Cell culture*. Four human RCC cell lines (786-O, Caki-1, Caki-2 and ACHN), obtained from the American Type Culture Collection (ATCC; Manassas, VI, USA), were cultured in RPMI-1640 medium (Wako Pure Chemical Industries, Ltd.) supplemented with 10% FBS (Thermo Fisher Scientific, Inc.), 100 U/ml penicillin G and 0.1 $\mu$g/ml streptomycin.

*siRNA and DNA transfection*. siRNA duplexes used to downregulate LAIR1 expression (LAIR1 stealth siRNA #1: HSS142792, LAIR1 stealth siRNA #2: HSS142794, LAIR1 stealth siRNA #3: HSS180495) and a negative control stealth siRNA duplex (#12935110) were purchased from Thermo Fisher Scientific, Inc. For all siRNA transfection studies, $5x10^4$ Caki-2 cells were seeded in a 12-well plate and 50 nM siRNA was transfected using Lipofectamine RNAiMAX reagent (Life Technologies; Thermo Fisher, Scientific, Inc.). For DNA transfection, $8x10^4$ ACHN cells were seeded in a 12-well plate 24 h before transfection. DNA transfection (1 $\mu$g) was performed using Lipofectamine® 2000 transfection reagent (Life Technologies; Thermo Fisher, Scientific, Inc.).

*Establishment of cell lines with stable LAIR1-FLAG expression*. The vector expressing LAIR1-FLAG (pcDNA3.1/LAIR1-FLAG) or empty vector (pcDNA3.1) was transfected into ACHN cells and cultured in a medium containing 2 mg/ml G418 (Roche, Basel, Switzerland) for selection.

*Water-soluble tetrazolium salt-8 (WST-8) cell proliferation assay*. Cell proliferation was examined by WST-8 assay. ACHN cells stably expressing LAIR1 or empty vector, or Caki-2 cells transfected with the LAIR1 siRNA or a negative control siRNA, were seeded in a 96-well plate ($0.05x10^4$ cells/well) and incubated for the indicated time. After incubation for 2 h with the WST-8 reagent (Dojindo Laboratories, Osaka, Japan) at 37˚C and 5% $CO_2$, the optical density was read at a wavelength of 450/630 nm (Ex/Em).

*Anchorage-independent cell proliferation assay*. Single cells were seeded into Nunclon Sphera 96F-well plates (Corning Inc., Corning, NY, USA) (ACHN cells: $0.4x10^4$ cells; Caki-2 cells: $0.8x10^4$ cells) in RPMI-1640 supplemented with 0.03% SphereMAX (Nissan Chemical Industries, Osaka, JAPAN), 10% FBS, 100 U/ml penicillin G and 0.1 $\mu$g/ml streptomycin. After 7 days, the spheres were stained with 10 $\mu$g/ml of calcein AM (BD Biosciences, Franklin Lakes, NJ, USA) and incubated for 30 min at 37ºC, 5% $CO_2$. Total sphere number was measured using the BZ-X800 fluorescence microscope at x20 magnification (Keyence Corp., Osaka, Japan).

*Wound healing assay*. Cells were seeded into a 24-well plate ($4.0x10^4$ cells/well) and incubated for 72 h at 37˚C, in 5% $CO_2$. A wound was created in a monolayer of ~90% confluent cells using a sterile 1-ml pipette tip. Cell images were recorded at 0 and 24 h for ACHN cells after wound creation using an Olympus IX71 fluorescence microscope at x40 magnification (Olympus Corp., Tokyo, Japan).

*Cell invasion assay*. The BioCoat Tumor Invasion system with the 8.0-$\mu$m pore size FluoroBlok membrane (Corning Inc.) was used to perform the cell invasion assay. Cells were seeded in the insert of 96-well plate ($2x10^4$ cells/well) in serum-free conditions, and medium supplemented with 10% FBS was used as a chemoattractant in the base plate. Following incubation for 12 h at 37˚C, in 5% $CO_2$, the cells were labeled with calcein AM (4 $\mu$g/ml), and the fluorescence of the invaded cells was read at a wavelength of 494/517 nm (Ex/Em).

*Establishment of LAIR1-FLAG stable cell-xenograft mice*. Nine female BALB/c nude mice were obtained from Oriental Yeast Co., Ltd. (Tokyo, Japan). Six-week-old mice were used for LAIR1-FLAG stable cell-xenograft mouse experiments. Animals were kept under a 12-h light/dark cycle at 22-24˚C in a pathogen-free mouse facility. Food and water were given *ad libitum*. ACHN-LAIR1-FLAG (LAIR1 #2) and ACHN-empty vector (mock) cells were both adjusted to a concentration of $1.0x10^7$ cells suspended in 50 $\mu$l serum-free RPMI-1640. The cell suspensions with 50 $\mu$l Matrigel (Corning Inc.) were then injected subcutaneously into the right flanks of the BALB/c nude mice (LAIR1 #2, N=4; mock #1, N=5). The tumor volume (V) was calculated as follows: $V = (\text{tumor length} \times \text{tumor width}^2)/2$. The weight of the mice was 20.68±1.4 g on day 32 after xenografts. All procedures were performed under a protocol approved by the Animal Experimentation Committee at Osaka University. Developed tumors were resected 32 days after xenografts. Mice were euthanized by overdose of isoflurane (2 times the anesthetic dose) for 5 min.

*Nanoparticle tracking analysis (NTA).* EV samples diluted with phosphate-buffered saline (PBS) (1:1,000 dilution) were analyzed with the NanoSight LM10 instrument (Quantum Design Japan, Tokyo, Japan) equipped with the NTA 2.0 analytical software (NanoSight Ltd., Malvern, UK). All measurements were performed under identical processing conditions (NTA 2.3 build 0034, Detection Threshold: 4 Multi, min Track Length: Auto, min Expected Size: Auto).

*Evaluation of RCC EVs on anchorage-dependent and anchorage-independent cell proliferation.* The EVs obtained from ACHN-LAIR1-FLAG (LAIR1 #2) or ACHN-empty vector (mock #1) cells (2 $\mu$g) were incubated with ACHN-empty vector (mock #1) cells and subjected to anchorage-dependent or anchorage-independent cell proliferation assays.

*Association of LAIR1 expression with patient prognosis.* Patients with no prognostic information were excluded and then the LAIR1 expression profiles were combined with the corresponding survival prognostic information. The prognostic value of each LAIR1 level was evaluated using a Kaplan-Meier curve and the log-rank method by GraphPad Prism 6.0 (GraphPad Software, Inc., La Jolla, CA, USA). Patients were divided into the high expression and low expression groups for each of the LAIR1 according to the mean value of the expression. Follow-up time was as follows. Overall survival: Median, 2,110 days (8-4,721 days); Progression-free survival: Median, 1,443.5 days (28-4,721 days).

*Statistical analysis.* Results are expressed as the mean ± standard deviation of the mean (SD). Differences between the values were statistically analyzed using the Student's t-test, paired t-test or one-way analysis of variance (ANOVA) with Tukey's post hoc tests (GraphPad Prism 6.0; GraphPad Software, Inc.). Association of clinical parameters with the LAIR1 mRNA level was tested by Mann-Whitney test. Overall survival and progression-free survival were calculated using the Kaplan-Meier method, and differences between groups were assessed by log-rank tests. A P-value of $<0.05$ was considered to indicate a statistically significant result.

## Results

*LAIR1 is enriched in RCC Te-EVs.* LC/MS analysis identified LAIR1 as aberrantly enriched in RCC Te-EVs compared to Te-EVs obtained from adjacent normal renal tissues (Fig. 1A). The mass spectrometric quantification results were further confirmed by western blot analysis (Fig. 1B). Transmission electron microscope (TEM) analysis illustrated that the isolated Te-EVs expressed LAIR1 on their surfaces (Fig. 1C). LAIR1 mRNA levels were significantly elevated in RCC tissues compared with the adjacent normal renal tissues (Fig. 1D and Table II). To investigate the LAIR1 function in RCC cells, we evaluated the LAIR1 protein expression in four RCC cell lines. Although the LAIR1 expression differed among the four cell lines, all cell lines expressed LAIR1 in whole cell lysates as well as in the EVs isolated from the cultured media (Fig. 1E). These results suggest that LAIR1 expression is elevated in RCC tissue, and that LAIR1 is secreted in extracellular vesicles (EVs) from RCC cells.

Table II. Statistical association of LAIR1 mRNA level with clinical parameters of the RCC patient tissues.

| Clinical parameters | n | LAIRI mRNA expression (median) | P-value (Mann-Whitney test) |
|---|---|---|---|
| TNM classification | | | 0.458 |
| I | 18 | 0.030 | |
| ≥II | 12 | 0.023 | |
| Pathological grade | | | 1.000 |
| ≤G2 | 17 | 0.026 | |
| ≥G3 | 13 | 0.030 | |
| Pathological stage | | | 0.796 |
| ≤pT1b | 19 | 0.028 | |
| ≥pT2a | 11 | 0.026 | |

LAIR1, leukocyte-associated immunoglobulin-like receptor 1; RCC, renal cell carcinoma; TNM, Tumor, Node, Metastasis.

*LAIR1 promotes cell proliferation in RCC cells.* To investigate the biological functions of LAIR1 in RCC cells, we first constructed ACHN cells stably overexpressing LAIR1 (Fig. 2A). LAIR1 overexpression upregulated both anchorage-dependent (Fig. 2B) and anchorage-independent (Fig. 2C) cell proliferation in ACHN cells. Moreover, although it did not significantly impact invasion ability (Fig. 2E), LAIR1 overexpression upregulated cell migration (Fig. 2D) in ACHN cells. Since LAIR1 siRNA #1 had no knockdown effect on LAIR1 protein levels, LAIR1 siRNA #2 and #3 were used for subsequent experiments (Fig. 2F). LAIR1 knockdown suppressed anchorage-dependent cell proliferation in Caki-2 cells (Fig. 2G).

To clarify the tumor-promoting potential of LAIR1 expression *in vivo*, ACHN cells stably expressing LAIR1 were xenografted into nude mice. These cells showed accelerated growth of tumor volume and increased tumor weight compared with empty vector-transfected ACHN cells (Fig. 2H and I), suggesting that increased LAIR1 expression upregulates RCC cell proliferation, leading to accelerated tumor growth.

*EV-LAIR1 has no significant effect on cell proliferation in RCC cells.* To elucidate whether RCC-derived EV-LAIR1 has the potential to upregulate RCC cell proliferation, we examined the biological effects of LAIR1-overexpressed EVs (LAIR1 #2 EVs) on RCC cells. EVs isolated from ACHN cells stably overexpressing LAIR1 were confirmed by western blot analysis using the well-defined EV marker CD81 (Fig. 3A). Nanoparticle tracking analysis showed that the isolated particles were under 200 nm in size and that there was no significant difference in secreted particle number between the mock vector-transfected ACHN cells and LAIR1-overexpressing ACHN cells (Fig. 3B and C). As shown in Fig. 3D and E, LAIR1 #2 EVs did not significantly impact either anchorage-dependent or anchorage-independent cell proliferation in empty vector-transfected ACHN cells (mock cells), suggesting that LAIR1 upregulates RCC cell

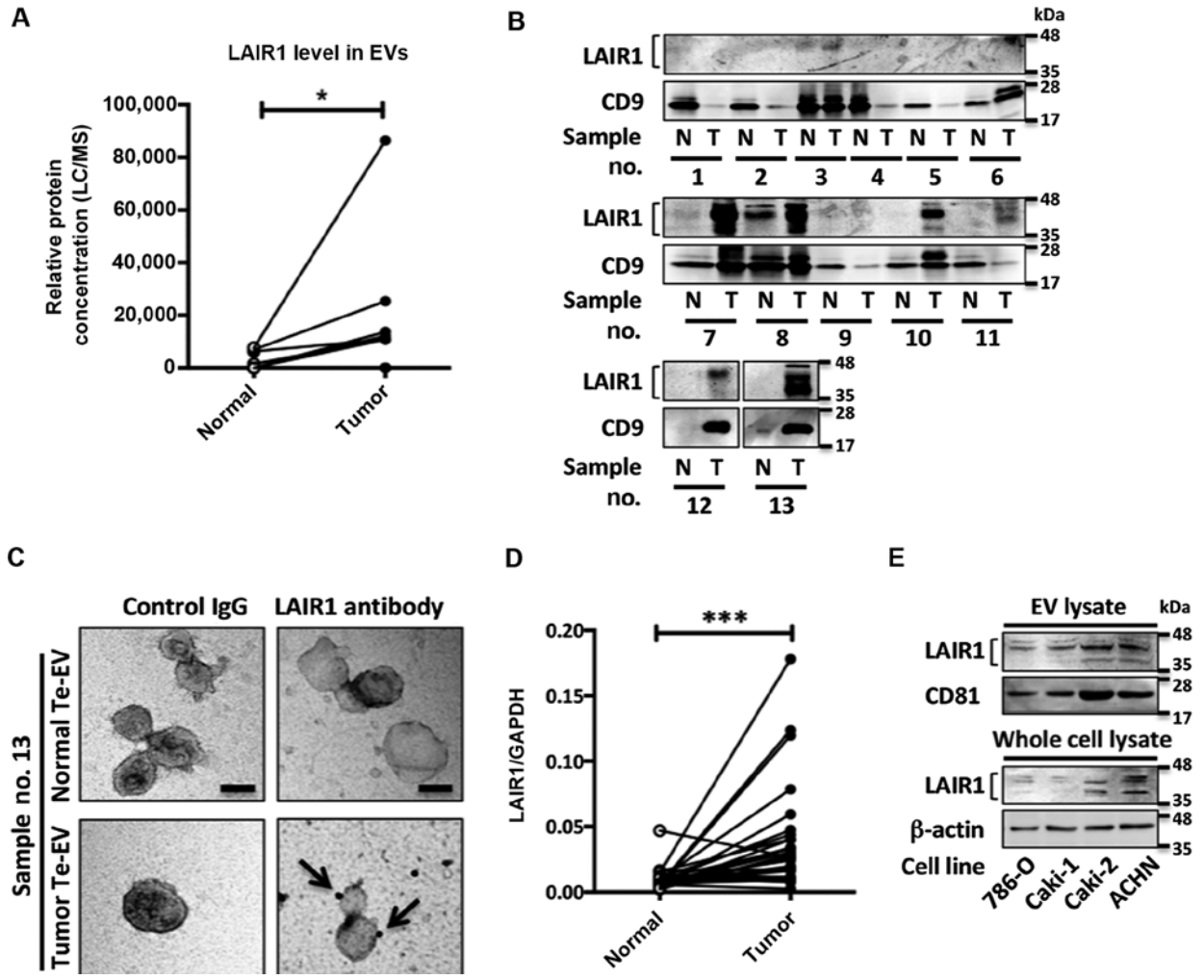


Figure 1. LAIR1 is enriched in RCC tissue-exudative EVs (Te-EVs). (A) A pairwise line chart for LAIR1 levels in Te-EVs is shown. *P<0.05 vs. normal Te-EVs. Paired t-test. (B) Upregulation of LAIR1 in tumor Te-EVs was confirmed by western blot analysis using 10 $\mu$g of EV samples per lane from 13 independent resected tissues. N, normal Te-EVs; T, tumor Te-EVs. (C) Te-EVs were analyzed by immunoelectron microscopy with anti-LAIR1 antibody. Mouse anti-LAIR1 antibody was detected with 20 nm colloidal gold nanoparticles (black arrows) coated with secondary antibody. Black scale bars, 100 nm. Sample No. 13 is presented. (D) LAIR1 mRNA expression was examined in 30 matched-pair RCC clinical samples by qPCR. Data are the relative expression normalized to GAPDH mRNA. ***P<0.001, Paired t-test. (E) Secreted EVs (5 $\mu$g) or whole lysates of RCC cell lines were subjected to western blot analysis. Representative results of three independent experiments are shown. RCC, renal cell carcinoma; LAIR1, leukocyte-associated immunoglobulin-like receptor 1; EVs, extracellular vesicles; Te-EVs, tissue-exudative extracellular vesicles.

proliferation irrespective of secreted EV-LAIR1. To examine whether LAIR1 was expressed not only in RCC cells but also in surrounding stromal cells, immunohistochemical staining was carried out on RCC tissues. Immunohistochemical staining revealed that RCC cells (Fig. 3F) and stromal cells (Fig. 3G) expressed LAIR1 in RCC tissues. Notably, stromal cells adjacent to RCC cells also expressed LAIR1 in RCC tissues (Fig. 3F, sample no. 15), suggesting that EV-LAIR1 secreted from RCC cells may be taken up by surrounding stromal cells.

*LAIR1 promotes cell proliferation via Akt in RCC cells.* Since the PI3K/Akt/mTOR pathway is a key hub for oncogenic processes including cell proliferation in RCC (17), we next examined the effect of LAIR1 on the PI3K/Akt/mTOR pathway. As shown in Fig. 4A, LAIR1 knockdown in Caki-2 cells decreased phosphorylation of Akt, whereas Erk1/2 and S6 kinase were not significantly affected. Moreover, in anchorage-independent growth systems, LAIR1 knockdown decreased the level of Akt phosphorylation in Caki-2 cells (Fig. 4B). On the other hand, LAIR1 overexpression upregulated the level of Akt phosphorylation in ACHN cells (Fig. 4C). To clarify the relationship between LAIR1 and Akt phosphorylation status, we evaluated the effect of the PI3K inhibitor (LY294002) on LAIR1-upregulated anchorage-independent cell proliferation. Although LY294002 significantly decreased the cell proliferation in empty vector-transfected ACHN cells, LAIR1 overexpression attenuated the effect of LY294002 on ACHN cells, suggesting that LAIR1 promotes cell proliferation via upregulation of Akt phosphorylation in RCC cells (Fig. 4D).

*High LAIR1 expression correlates with poor progression-free survival in RCC.* Finally, Kaplan-Meier survival curve analyses were performed in RCC patients. These curves indicated that high expression of LAIR1 mRNA in RCC tissue was associated with poor progression-free survival (Fig. 5).

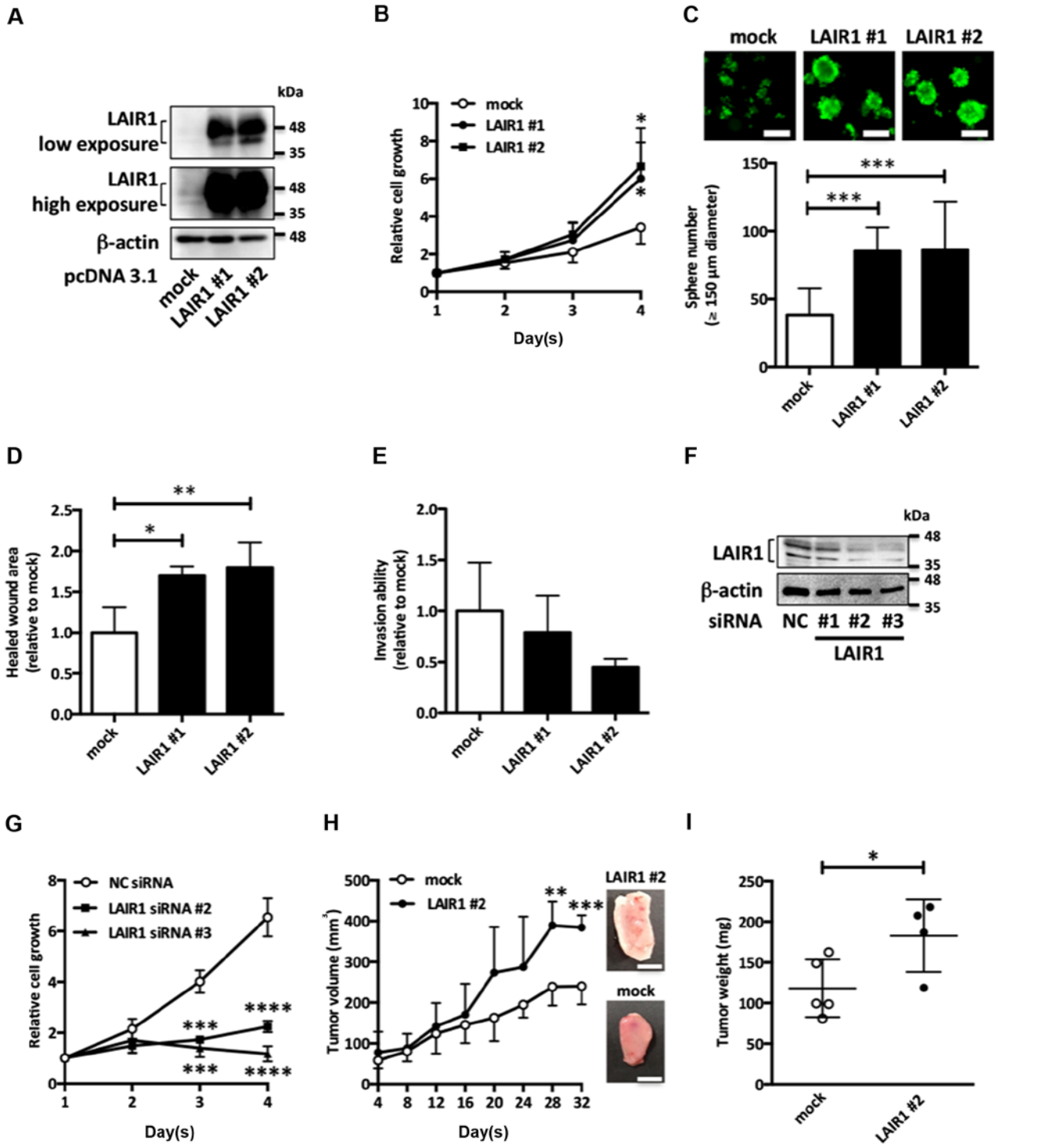


Figure 2. LAIR1 overexpression promotes tumorigenesis in RCC. (A) ACHN cells stably overexpressing LAIR1-FLAG were subjected to western blot analysis. Representative results of three independent experiments are shown. ACHN cells stably overexpressing LAIR1-FLAG (LAIR1 #1, LAIR1 #2) or control cells (mock) were examined in anchorage-dependent (B) and anchorage-independent (C) cell proliferation assays. Values are the mean ± SD of six independent experiments. $^{*}$P<0.05, $^{***}$P<0.001 vs. mock. One-way ANOVA. White scale bars, 150 $\mu$m. (D) Cell motility was measured 24 h after wound formation by scraping in serum-free conditions. The results are expressed as mean ± SD of four independent experiments. $^{*}$P<0.05, $^{**}$P<0.01 vs. mock. One-way ANOVA. (E) The cell suspension was added to the upper chamber of Matrigel-coated Transwell membrane inserts, and the lower chamber was filled with the medium and then cultured for 12 h. Fluorescence derived from invasive cells was measured. Values are mean ± SD of four independent experiments. (F) Caki-2 cells transfected with negative control (NC) siRNA or LAIR1 siRNA were subjected to western blot analysis. Representative results of three independent experiments are shown. (G) Caki-2 cells transfected with LAIR1 siRNA were examined in anchorage-dependent cell proliferation assays. Values are the mean ± SD of three independent experiments. $^{***}$P<0.001, $^{****}$P<0.0001 vs. NC siRNA. One-way ANOVA. (H) ACHN cells stably overexpressing LAIR1-FLAG (LAIR1 #2, N=4) and control ACHN cells (mock, N=5) were injected into nude mice. Tumor size was measured and calculated every four days. The values are presented as the mean ± SD for each group. $^{**}$P<0.01, $^{***}$P<0.001 vs. control tumor. t-test. Representative xenograft tumor images (upper position: LAIR1 #2, lower position: mock) are shown. Maximum tumor volume and diameter of resected tumors was as follows. Mock: 304.2 mm$^3$, 10.5 mm; LAIR1 #2: 416.3 mm$^3$, 15.1 mm. There were no multiple tumors on xenografted mouse. White scale bar, 5 mm. (I) Tumor weight for mock and LAIR1 #2 xenografted mice. The values are presented as the mean ± SD for each group. $^{*}$P<0.05 vs. control tumor. t-test. RCC, renal cell carcinoma; LAIR1, leukocyte-associated immunoglobulin-like receptor 1.

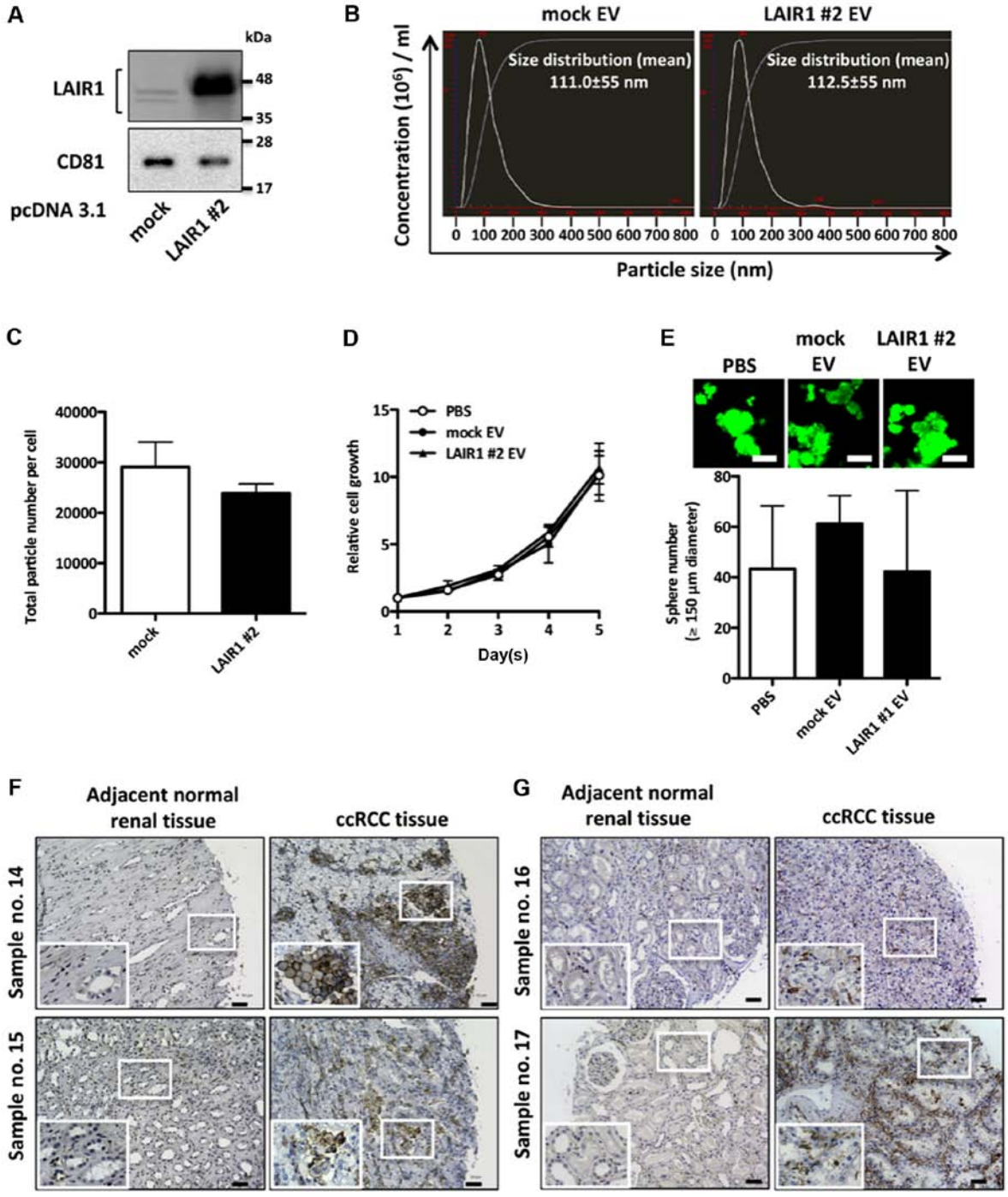


Figure 3. EV-LAIR1 secreted from RCC cells had no significant effect on cell proliferation in ccRCC cells. (A) EVs were isolated from ACHN cells stably overexpressing LAIR1-FLAG (LAIR1 #2) or control cells (mock) and analyzed by western blot analysis using anti-LAIR1 and anti-CD81 antibodies. Representative results of three independent experiments are shown. (B) EVs were subjected to nanoparticle tracking analysis. Representative results of three independent experiments are shown. (C) Total EV particle number per cell. The values are presented as the mean ± SD for each group. (D) Control cells (mock) were seeded on a 96 well plate and treated with EVs (10 $\mu$g/ml) isolated from cultured media of mock or LAIR1 #2 followed by WST-8 assay at the indicated time- points. The values are presented as the mean ± SD of three independent experiments. (E) Control cells (mock) were seeded on a Nunclon Sphera 96F-well plate and treated with EVs (10 $\mu$g/ml) isolated from cultured media of mock or LAIR1 #2 cells for 7 days. Values presented as mean ± SD of three independent experiments. White scale bars, 150 $\mu$m. (F and G) The expression of LAIR1 in RCC specimens was examined by immunohistochemical staining. Black scale bars, 50 $\mu$m. EVs, extracellular vesicles; ccRCC, clear cell renal cell carcinoma; LAIR1, leukocyte-associated immunoglobulin-like receptor 1.

## Discussion

In the present study, we identified aberrant LAIR1 overexpression as a consequential factor in the development of renal cell carcinoma (RCC). A receptor widely expressed on immune cells, leukocyte-associated immunoglobulin-like receptor 1 (LAIR1) has previously been reported to play a role in leukemia, with multiple studies indicating that blocking LAIR1 activation in leukemia cells decreases cell proliferation. Poggi *et al* demonstrated that in B-cell chronic lymphocyte leukemia cells, antibody engagement with LAIR1 blocks the activation of Akt and NF-κB leading to decreased cell proliferation (18)

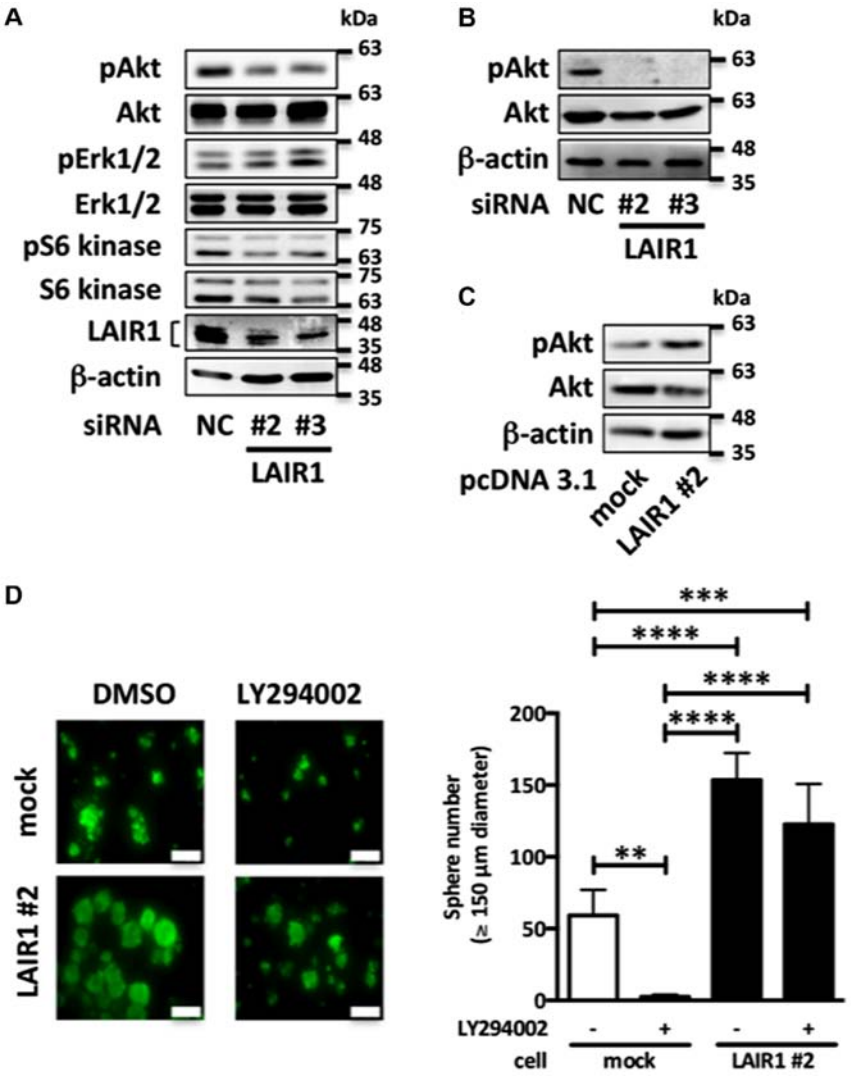


Figure 4. LAIR1 promotes cell proliferation via Akt phosphorylation in RCC cells. (A) Protein lysates from Caki-2 cells transfected with negative control (NC) siRNA or LAIR1 siRNA #2 and #3 for 48 h under anchorage-dependent condition were subjected to western blot analysis. Representative results of three independent experiments are shown. (B) Protein lysates from Caki-2 cells transfected with negative control (NC) siRNA or LAIR1 siRNAs for 7 days under anchorage-independent condition were subjected to western blot analysis. Representative results of three independent experiments are shown. (C) Protein lysate from ACHN cells stably overexpressing LAIR1-FLAG (LAIR1 #2) or control ACHN cells (mock) cultured under anchorage-independent conditions for 7 days were subjected to western blot analysis. Representative results of three independent experiments are shown. (D) ACHN cells stably overexpressing LAIR1-FLAG (LAIR1 #2) or control ACHN cells (mock) were cultured under anchorage-independent conditions for 7 days with LY294002 (1 $\mu$M) or DMSO. Representative results of three independent experiments are shown. Values presented as mean ± SD of four independent experiments. $^{**}$P<0.01, $^{***}$P<0.001, $^{****}$P<0.0001 vs. mock without LY294002. One-way ANOVA. White scale bars, 150 $\mu$m. LAIR1, leukocyte-associated immunoglobulin-like receptor 1; RCC, renal cell carcinoma; DMSO, dimethyl sulfoxide.

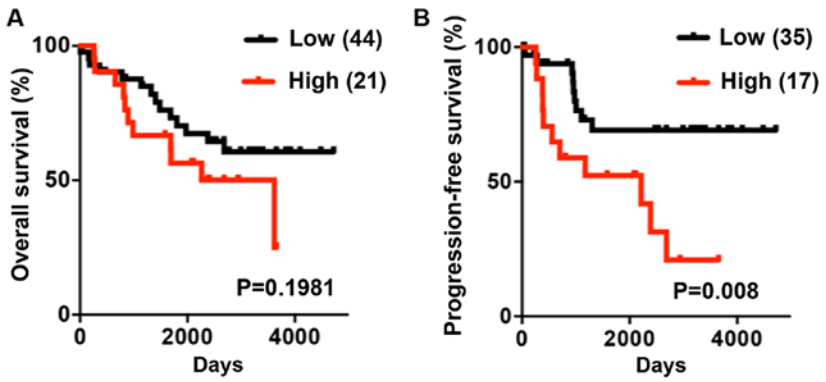


Figure 5. Association of LAIR1 mRNA expression levels with overall survival and progression-free survival. (A) Overall survival. RCC tissue samples were divided into two groups according to LAIR1 mRNA expression: Low (44 samples) and high (11 samples). The high- and low LAIR1 subgroups were divided using the mean level of LAIR1. (B) Progression-free survival. RCC tissue samples were divided into two groups according to LAIR1 mRNA expression: Low (35 samples) and high (17 samples). Log-rank test. LAIR1, leukocyte-associated immunoglobulin-like receptor 1; RCC, renal cell carcinoma.

and Kang *et al* showed that LAIR1 knockdown significantly inhibited *in vitro* and *in vivo* cell growth in human leukemia cell lines (19). These findings are consistent with our current study, which shows that siRNA knockdown of LAIR1 reduced cell proliferation via suppression of Akt phosphorylation in RCC cells. Moreover, Kang *et al* revealed that LAIR1 deficiency exhausted tumor-initiating cells via apoptosis in mouse acute myeloid leukemia cells. Our data showed that LAIR1 promotes anchorage-independent cell proliferation activity, which represents one of the key features of cancer stem cells. LAIR1 upregulated Akt phosphorylation, which leads to cancer stem cell activation and promotes tumor development in RCC (20,21). Therefore, LAIR1 may regulate cell proliferation by activating cancer stem cells via upregulation of Akt phosphorylation in RCC.

In addition to leukocyte Ig-like receptor subfamily B (LILRB)2, LILRB4 (22,23), which contains identical domain organization to LAIR1, LAIR1 has been shown to have tumor-promoting roles in leukemia (19) and RCC cells. SHP-1, which directly binds to the ITIM region of LAIR1 and transfers the signal downstream, is known to act as either an oncogene or as a tumor suppressor depending on the type of cancer (24). In RCC, inhibition of SHP-1 significantly decreased the proliferation of RCC cell lines (25). Moreover, SHP-1 inhibition downregulated the phosphorylation status of Akt in RCC cells, suggesting that downstream of LAIR1, SHP-1 acts as an oncogene in RCC cells leading to upregulation of Akt phosphorylation.

Although we performed flow cytometric analysis, we could not detect LAIR1 on the cell surface in RCC cell lines (data not shown). Our IHC data (Fig. 3F) and the IHC data from the public database (The Human Protein Atlas) show both membranous and cytoplasmic staining of LAIR1 in RCC cells. In ovarian cancer cells, the localization of LAIR1 was dependent on cell lines. LAIR-1 proteins were localized on both the plasma membrane and in the cytoplasm of COC1 cells, while predominately localized in the cytoplasm of HO8910 cells (26). Moreover, LAIR1 knockdown affected the cell proliferation in HO8910 cells, where LAIR1 was localized in the cytoplasm (26). Therefore, although the underlying mechanism is unclear, we think that LAIR1 may localize in the cytosol and promote tumorigenesis in RCC cells.

Some of the tissue-exudative extracellular vesicles (Te-EVs) obtained from normal renal tissue showed high CD9 expression compared to those in RCC Te-extracellular vesicles (EVs). In our previous study (5), we found that most of tetraspanins including CD9 were often downregulated in tumor-derived EVs compared to those in normal-derived EVs. Moreover, Kwon *et al* showed that 54% of RCC patients had low CD9 expression (27). Therefore, the low CD9 expression in RCC Te-EVs may be due to the CD9 expression pattern in RCC tissue.

We initially identified LAIR1 as a protein enriched in RCC-derived Te-EVs. Since overexpression of LAIR1 accelerated tumor growth *in vivo*, we investigated whether treatment of RCC cells with EV-LAIR1 isolated from RCC EVs were sufficient to affect cell proliferation. Our data indicated that incubation of RCC cells with EV-LAIR1 had little direct effect on proliferation. EVs are one of the tools by which cancer cells communicate with themselves, other cell types (e.g., vascular endothelial cells, immune cells and fibroblast), and the surrounding supportive structures constituting the tumor microenvironment (28). It is becoming increasingly apparent that the contents of EVs may endow them with potent reprogramming capacity for manipulating recipient cells (29-32). In renal cancer, Grange *et al* (33) reported that renal cancer cells secrete EVs, which activate vascular endothelial cells to organize capillary-like structures and induce enhanced chemoresistance. Our data showed that not only RCC cells but also stromal cells adjacent to RCC were LAIR1-positive (Fig. 3F), suggesting that EV-LAIR1 secreted from RCC cells may influence the tumor microenvironment and lead to accelerated tumor growth. Although our *in vivo* xenograft model could not address the effect of EV-LAIR1 on tumor microenvironment including immune cells, further studies using mouse allograft model may solve this issue.

In conclusion, the present study showed that LAIR1 was secreted in EVs from RCC cells, and that LAIR1 intracellular signaling enhanced Akt phosphorylation, leading to accelerated tumor growth in RCC cells.

**Acknowledgements**

We thank Dr Eiji Oiki (Graduate School of Medicine, Osaka University) for the technical assistance for the TEM analysis.

**Funding**

The present study was supported by the Project for Cancer Research and Therapeutic Evolution from the Japan Agency for Medical Research and Development (AMED) to KU under grant no. 18cm0106405h0003.

**Availability of data and materials**

The datasets used and/or analyzed during the current study are available from the corresponding author on reasonable request.

**Author contributions**

KJ, MU and KU were involved in the conception and design of the study; KJ, MU, KT, KU and NN were involved in the data collection; KJ, MU, KN, YH, CW, YI, YY, TH, ToK, KM, TaK, AK, TU, AN, KF and KU were involved in the data analysis; KJ, MU and KU conducted the investigative experiments; MU, KU and NN were involved in the project administration; MU, KT and NN supervised the study; KJ, MU and KF wrote and edited the manuscript. All authors read and approved the manuscript and agree to be accountable for all aspects of the research in ensuring that the accuracy or integrity of any part of the work are appropriately investigated and resolved.

**Ethics approval and consent to participate**

Written informed consent was obtained from each patient, and the study was approved by the ethics review board of the Osaka University Medical Hospital.

## Patient consent for publication

Informed consent was obtained from all participants included in the study.

## Competing interests

NN reports receiving commercial research grants from Takeda Pharmaceutical, Novartis Pharma, and Astra Zeneca. No potential conflicts of interest were disclosed by the other authors.

## References


1. Jonasch E, Futreal PA, Davis IJ, Bailey ST, Kim WY, Brugarolas J, Giaccia AJ, Kurban G, Pause A, Frydman J, *et al*: State of the science: An update on renal cell carcinoma. Mol Cancer Res 10: 859-880, 2012.
2. Nerich V, Hugues M, Paillard MJ, Borowski L, Nai T, Stein U, Nguyen Tan Hon T, Montcuquet P, Maurina T, Mouillet G, *et al*: Clinical impact of targeted therapies in patients with metastatic clear-cell renal cell carcinoma. Onco Targets Ther 7: 365-374, 2014.
3. Mickisch GH: Principles of nephrectomy for malignant disease. BJU Int 89: 488-495, 2002.
4. Kalluri R: The biology and function of exosomes in cancer. J Clin Invest 126: 1208-1215, 2016.
5. Jingushi K, Uemura M, Ohnishi N, Nakata W, Fujita K, Naito T, Fujii R, Saichi N, Nonomura N, Tsujikawa K, *et al*: Extracellular vesicles isolated from human renal cell carcinoma tissues disrupt vascular endothelial cell morphology via azurocidin. Int J Cancer 124: 607-617, 2018.
6. Meyaard L, Adema GJ, Chang C, Woollatt E, Sutherland GR, Lanier LL and Phillips JH: LAIR-1, a novel inhibitory receptor expressed on human mononuclear leukocytes. Immunity 7: 283-290, 1997.
7. Poggi A, Pella N, Morelli L, Spada F, Revello V, Sivori S, Augugliaro R, Moretta L and Moretta A: p40, a novel surface molecule involved in the regulation of the non-major histocompatibility complex- restricted cytolytic activity in humans. Eur J Immunol 25: 369-376, 1995.
8. Poggi A, Tomasello E, Ferrero E, Zocchi MR and Moretta L: p40/LAIR-1 regulates the differentiation of peripheral blood precursors to dendritic cells induced by granulocyte-monocyte colony-stimulating factor. Eur J Immunol 28: 2086-2091, 1998.
9. Florian S, Sonneck K, Czerny M, Hennersdorf F, Hauswirth AW, Bühring HJ and Valent P: Detection of novel leukocyte differentiation antigens on basophils and mast cells by HLDA8 antibodies. Allergy 61: 1054-1062, 2006.
10. Verbrugge A, De Ruiter T, Geest C, Coffer PJ and Meyaard L: Differential expression of leukocyte-associated Ig-like receptor-1 during neutrophil differentiation and activation. J Leukoc Biol 79: 828-836, 2006.
11. Maasho K, Masilamani M, Valas R, Basu S, Coligan JE and Borrego F: The inhibitory leukocyte-associated Ig-like receptor-1 (LAIR-1) is expressed at high levels by human naive T cells and inhibits TCR mediated activation. Mol Immunol 42: 1521-1530, 2005.
12. Lebbink RJ, De Ruiter T, Kaptijn GJ, Bihan DG, Jansen CA, Lenting PJ and Meyaard L: Mouse leukocyte-associated Ig-like receptor-1 (mLAIR-1) functions as an inhibitory collagen-binding receptor on immune cells. Int Immunol 19: 1011-1019, 2007.
13. Nishida-Aoki N, Tominaga N, Takeshita F, Sonoda H, Yoshioka Y and Ochiya T: Disruption of circulating extracellular vesicles as a novel therapeutic strategy against cancer metastasis. Mol Ther 25: 181-191, 2017.
14. Yoshioka Y, Kosaka N, Konishi Y, Ohta H, Okamoto H, Sonoda H, Nonaka R, Yamamoto H, Ishii H, Mori M, *et al*: Ultra-sensitive liquid biopsy of circulating extracellular vesicles using ExoScreen. Nat Commun 5: 3591, 2014.
15. Fuhrman SA, Lasky LC and Limas C: Prognostic significance of morphologic parameters in renal cell carcinoma. Am J Surg Pathol 6: 655-663, 1982.
16. Lässer C, Eldh M and Lötvall J: Isolation and characterization of RNA-containing exosomes. J Vis Exp 9: e3037, 2012.
17. Guo H, German P, Bai S, Barnes S, Guo W, Qi X, Lou H, Liang J, Jonasch E, Mills GB and Ding Z: The PI3K/AKT pathway and renal cell carcinoma. J Genet Genomics 42: 343-353, 2015.
18. Poggi A, Catellani S, Bruzzone A, Caligaris-Cappio F, Gobbi M and Zocchi MR: Lack of the leukocyte-associated Ig-like receptor-1 expression in high-risk chronic lymphocytic leukaemia results in the absence of a negative signal regulating kinase activation and cell division. Leukemia 22: 980-988, 2008.
19. Kang X, Lu Z, Cui C, Deng M, Fan Y, Dong B, Han X, Xie F, Tyner JW, Coligan JE, *et al*: The ITIM-containing receptor LAIR1 is essential for acute myeloid leukaemia development. Nat Cell Biol 17: 665-677, 2015.
20. Khan MI, Czarnecka AM, Lewicki S, Helbrecht I, Brodaczewska K, Koch I, Zdanowski R, Król M and Szczylik C: Comparative gene expression profiling of primary and metastatic renal cell carcinoma stem cell-like cancer cells. PLoS One 11: e0165718, 2016.
21. Xia P and Xu XY: PI3K/Akt/mTOR signaling pathway in cancer stem cells: From basic research to clinical application. Am J Cancer Res 5: 1602-1609, 2015.
22. Khan MF, Bahr JM, Yellapa A, Bitterman P, Abramowicz JS, Edassery SL, Basu S, Rotmensch J and Barua A: Expression of leukocyte inhibitory immunoglobulin-like transcript 3 receptors by ovarian tumors in laying hen model of spontaneous ovarian cancer. Transl Oncol 5: 85-91, 2012.
23. Liu X, Yu X, Xie J, Zhan M, Yu Z, Xie L, Zeng H, Zhang F, Chen G, Yi X and Zheng J: ANGPTL2/LILRB2 signaling promotes the propagation of lung cancer cells. Oncotarget 6: 21004-21015, 2015.
24. Kang X, Kim J, Deng M, John S, Chen H, Wu G, Phan H and Zhang CC: Inhibitory leukocyte immunoglobulin-like receptors: Immune checkpoint proteins and tumor sustaining factors. Cell Cycle 15: 25-40, 2016.
25. Tao T, Yang X, Zheng J, Feng D, Qin Q, Shi X, Wang Q, Zhao C, Peng Z, Liu H, *et al*: PDZK1 inhibits the development and progression of renal cell carcinoma by suppression of SHP-1 phosphorylation. Oncogene 36: 6119-6131, 2017.
26. Cao Q, Fu A, Yang S, He X, Wang Y, Zhang X, Zhou J, Luan X, Yu W and Xue J: Leukocyte-associated immunoglobulin-like receptor-1 expressed in epithelial ovarian cancer cells and involved in cell proliferation and invasion. Biochem Biophys Res Commun 458: 399-404, 2015.
27. Kwon HJ, Min SY, Park MJ, Lee C, Park JH, Chae JY and Moon KC: Expression of CD9 and CD82 in clear cell renal cell carcinoma and its clinical significance. Pathol Res Pract 210: 285-290, 2014.
28. Kosaka N, Yoshioka Y, Fujita Y and Ochiya T: Versatile roles of extracellular vesicles in cancer. J Clin Invest 126: 1163-1172, 2016.
29. Al-Nedawi K, Meehan B, Micallef J, Lhotak V, May L, Guha A and Rak J: Intercellular transfer of the oncogenic receptor EGFRvIII by microvesicles derived from tumour cells. Nat Cell Biol 10: 619-624, 2008.
30. Yokoi A, Yoshioka Y, Yamamoto Y, Ishikawa M, Ikeda SI, Kato T, Kiyono T, Takeshita F, Kajiyama H, Kikkawa F, *et al*: Malignant extracellular vesicles carrying *MMP1* mRNA facilitate peritoneal dissemination in ovarian cancer. Nat Commun 8: 14470, 2017.
31. Song X, Ding Y, Liu G, Yang X, Zhao R, Zhang Y, Zhao X, Anderson GJ and Nie G: Cancer cell-derived exosomes induce mitogen-activated protein kinase-dependent monocyte survival by transport of functional receptor tyrosine kinases. J Biol Chem 291: 8453-8464, 2016.
32. Webber J, Steadman R, Mason MD, Tabi Z and Clayton A: Cancer exosomes trigger fibroblast to myofibroblast differentiation. Cancer Res 70: 9621-9630, 2010.
33. Grange C, Tapparo M, Collino F, Vitillo L, Damasco C, Deregibus MC, Tetta C, Bussolati B and Camussi G: Microvesicles released from human renal cancer stem cells stimulate angiogenesis and formation of lung premetastatic niche. Cancer Res 71: 5346-5356, 2011.